

The effect of two dimensions on the temperature variation of displacement-displacement autocorrelation function, second-order Doppler shift and specific heat in graphite

This article has been downloaded from IOPscience. Please scroll down to see the full text article.

1989 J. Phys.: Condens. Matter 1 7535

(<http://iopscience.iop.org/0953-8984/1/41/004>)

View [the table of contents for this issue](#), or go to the [journal homepage](#) for more

Download details:

IP Address: 171.66.16.96

The article was downloaded on 10/05/2010 at 20:28

Please note that [terms and conditions apply](#).

The effect of two dimensions on the temperature variation of displacement–displacement autocorrelation function, second-order Doppler shift and specific heat in graphite

S P Tewari and Poonam Silotia

Department of Physics and Astrophysics, University of Delhi, Delhi-110 007, India

Received 14 March 1989, in final form 16 May 1989

Abstract. A model for the frequency-distribution function of phonons in graphite that explicitly takes into account the presence of two-dimensional modes has been used to explain successfully (i) the recently observed temperature-dependent displacement–displacement autocorrelation function perpendicular to the basal plane $\langle u_z^2 \rangle$ in the temperature range 5–300 K, (ii) the measured specific heat in the temperature range 10–300 K and (iii) the observed second-order Doppler shift in the temperature range 293–743 K. It is found that the two dimensional modes play a dominant role over the entire temperature range. Calculations based on other anisotropic models for $\langle u_z^2 \rangle$ have also been made and compared.

1. Introduction

Recently, using x-ray reflection, the experimental values of displacement–displacement autocorrelation function, i.e. the mean-square vibrational amplitude, of bulk atoms of graphite normal to the basal plane have been reported in the temperature range 300–5 K [1]. As the temperature is decreased from 300 K, the mean-square vibrational amplitude, as expected, is found to decrease and at very low temperatures approaches a finite minimum value caused by zero-point vibrations of the atoms.

Graphite, as is well known, is an outstanding example of a layered crystal; therefore, to interpret these results in terms of an isotropic three-dimensional Debye distribution function of phonons is physically unacceptable [1]. Even at very low temperatures, where essentially low-energy elastic modes are excited and dispersion is absent, the Debye approximation in such an anisotropic crystal is valid to the extent that the distribution function is of the type $g(\nu) = A\nu^2$ only over a limited range of ν and not over the entire frequency range up to $\nu_{\max} = \nu_D$. Here ν is the phonon frequency [2–4]. Further, the constant A does not, therefore, correspond to the ordinary value $9N/(k_B\theta_D)^3$ that comes about when all the total number of $3N$ modes are of ν^2 type from zero to $\nu_{\max}(h\nu_D = k_B\theta_D)$. Hsieh and Colella [1], in analysing their experimental results, have used the three-dimensional isotropic Debye phonon-distribution function over the entire frequency range up to ν_D , and this distribution function has been used to evaluate mean-square displacements (MSD) in the temperature range 300–5 K. It was, therefore, natural that their calculated values of the MSD, particularly at low temperatures, were

higher than the experimental values, and the difference between the two was a maximum at 0 K. Further, using these results and assuming that, at low temperatures, the thermal vibrations are strongly anisotropic, they obtained the value of α equal to 0.89 for the bulk atoms of graphite. (The value of α less than one represents the degree of anisotropy in the MSD of the atoms.) Such a result is quite unacceptable for the bulk atoms of graphite because the MSD perpendicular to the basal plane would continue to be anisotropic at all the temperatures and not merely at low temperatures. In other words, since the crystal structure of graphite does not change with increase in temperature and the force field under which a given atom vibrates continues to be anisotropic as it is at low temperatures [5], the vibrations would continue to be anisotropic at all the temperatures. In fact, using three-dimensional isotropic Debye distribution function of phonons, they can just represent the approximate values of their observed MSD without giving any clue regarding the anisotropic nature of the observed MSD [6, 7].

The elastic anisotropy of graphite is evident, besides not only from its crystal structure, but also from the low-temperature specific heat variation. It is well known that the measured values of specific heat of graphite at very low temperatures $T < 2$ K varies as T^3 and at low temperatures, i.e. temperature range of approximately 15–80 K it varies as T^2 rather than T^3 [8, 9]. In order to explain this behaviour of the specific heat, a few dynamical models for the phonon frequency distribution function for graphite have been suggested [2, 3]. These phonon frequency-distribution functions can be used to study the anisotropic MSD of graphite.

2. Mathematical formalism

We suggest an anisotropic dynamical model for the phonon frequency-distribution function of graphite somewhat similar to that suggested by Krumhansl and Brooks [2], who solved the appropriate dynamical matrix for the normal-mode frequencies of a graphite atom vibrating parallel to the c axis. The phonon frequency-distribution function has a region of linear ν dependence. Recently Boato and co-workers [10] have obtained a frequency-distribution function of phonons for the surface atoms of graphite vibrating perpendicular to the surface assuming the dispersion relation for the phonons suggested by Komatsu [3]. Their frequency-distribution function also carries a region where the dependence of $g(\nu)$ with ν is linear, indicating the planar nature of vibrations. Very recently similar models have been employed to study the various physical properties of predominantly anisotropic two-dimensional [11, 12] and one-dimensional [13, 14] solids.

2.1. Dynamical model

We suggest a dynamical model in which the elastic dynamical modes in a given direction i are given as follows:

$$\begin{aligned} g_i(\nu) &= A_i \nu_i^2 & 0 \leq \nu \leq \nu_{0i} \\ &= B_i \nu_i & \nu_{0i} \leq \nu \leq \nu_{mi} \\ &= 0 & \nu > \nu_{mi} \end{aligned} \quad (1)$$

the values of A_i and B_i are determined by the conditions:

- (i) the distribution function has to be continuous at $\nu = \nu_{0i}$; and
(ii) the total number of modes should be equal to N . The characteristic frequencies ν_{0i} and ν_{mi} are determined using appropriate experimental data.

2.2. Atomic mean-square displacement

Mean-square displacement in a given direction i in terms of the phonon frequency distribution function is given as follows:

$$\langle u_i^2 \rangle = \frac{\hbar}{MN} \int_0^{\nu_{mi}} \nu^{-1} g_i(\nu) \left[\frac{1}{2} + \frac{1}{\exp(h\nu/k_B T) - 1} \right] d\nu. \quad (2)$$

Using $g_i(\nu)$ from expression (1) in (2), we get

$$\begin{aligned} \langle u_i^2 \rangle = & \frac{\hbar^2}{Mk_B} \frac{\Delta_i}{\theta_{0i}} \left[\left(\frac{1}{\delta_i} - \frac{1}{2} \right) + 2 \left(\frac{T}{\theta_{0i}} \right)^2 \int_0^{\theta_{0i}/T} \frac{x}{(e^x - 1)} dx \right. \\ & \left. + 2 \left(\frac{T}{\theta_{0i}} \right) \int_{\theta_{0i}/T}^{\theta_{mi}/T} \frac{1}{(e^x - 1)} dx \right] \end{aligned} \quad (3)$$

where $\delta_i = \theta_{0i}/\theta_{mi}$ and $\Delta_i = (1/\delta_i^2 - \frac{1}{3})^{-1}$.

Here k_B is the Boltzmann constant, and M is the mass of graphite atom, $i = z$ gives the direction parallel to the c axis, i.e., \perp to the basal plane. $i = x, y$ gives the direction perpendicular to the c axis, i.e. in the basal plane.

On the basis of Krumhansl and Brooks (KB) model [2], the expression for MSD along the direction i is given as

$$\begin{aligned} \langle u_i^2 \rangle = & \frac{\hbar^2}{2Mk_B} \left[\frac{3n_i}{2\theta_{0i}} + \frac{2(1-n_i)}{\theta_{mi} + \theta_{0i}} + \frac{6n_i}{\theta_{0i}^3} T^2 \int_0^{\theta_{0i}/T} \frac{x}{(e^x - 1)} dx \right. \\ & \left. + \frac{4(1-n_i)}{(\theta_{mi}^2 - \theta_{0i}^2)} T \int_{\theta_{0i}/T}^{\theta_{mi}/T} \frac{1}{(e^x - 1)} dx \right] \end{aligned} \quad (4)$$

where n_i is the fraction of modes in the direction i .

Chen and Yiu [4], using the anisotropic phonon frequency-distribution function of graphite, derived by Komatsu [3], gave the following expression for the temperature variation of MSD of graphite atoms parallel to the c axis, i.e. $i = z$:

$$\langle u_z^2 \rangle = 291.08 \text{ MeV}^{-2} F(T) \quad (5)$$

where $F(T)$ is a complicated function of temperature and for $T > 42$ K reduces to the following expression:

$$F(T) = 3.344 \times 10^{-2} T - 354.3 T^{-1} - 1.586 \times 10^4 T^{-3} + 1.585 \times 10^7 T^{-5} + \dots \quad (6)$$

2.3. Second-order Doppler shift

Making use of the suggested dynamical model, the expression for the temperature-dependent second-order Doppler shift (SOD), δ_T , which is related to the velocity-velocity autocorrelation function is given as follows:

$$\begin{aligned} \delta_{T,i} = & \frac{3k_B}{Mc(3\theta_{mi}^2 - \theta_{0i}^2)} \left[\left(\frac{4\theta_{mi}^3 - \theta_{0i}^3}{24} \right) + \frac{T^4}{\theta_{0i}} \int_0^{\theta_{0i}/T} \frac{x^3}{(e^x - 1)} dx \right. \\ & \left. + T^3 \int_{\theta_{0i}/T}^{\theta_{mi}/T} \frac{x^2}{(e^x - 1)} dx \right]. \end{aligned} \quad (7)$$

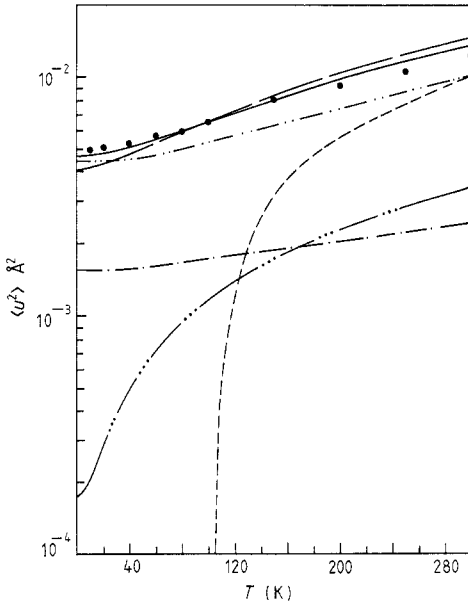


Figure 1. Mean-square displacement of the bulk atom of graphite normal to the basal plane. ● represents the experimental points and the rest are the calculated results based on different models. --- KB model; - · - · - Chen and Yiu; — our model. · · · · and · · · · · show respectively the two-dimensional and three-dimensional contributions to MSD along the *c* axis based on our model. Also shown are the values of MSD in the basal plane using our model — · — ·.

2.4. Specific heat

In the present model, the total specific heat, C_V , takes the following form

$$C_V = 2C_{V_{xy}} + C_{V_z}$$

where $C_{V_{xy}}$ and C_{V_z} denote respectively the specific heat of *xy*-modes and *z*-modes. The expression for any one of these modes is given as follows:

$$C_{Vi} = \frac{6RT^3}{\theta_{0i}(3\theta_{mi}^2 - \theta_{0i}^2)} \int_0^{\theta_{0i}/T} \frac{x^4 e^x}{(e^x - 1)^2} dx + \frac{6RT^2}{(3\theta_{mi}^2 - \theta_{0i}^2)} \int_{\theta_{0i}/T}^{\theta_{mi}/T} \frac{x^3 e^x}{(e^x - 1)^2} dx. \quad (8)$$

3. Results and discussion

We have calculated the MSD using Chen and Yiu's expression (5) in the temperature range 300–105 K. Below 105 K, the calculated values of MSD become negative, which is unphysical. The calculated values in the temperature range 105–300 K are plotted in figure 1. As the temperature increases from 105 K, the MSD sharply increases from its low value up to about 180 K, beyond which the increase becomes somewhat slower. In most of the temperature range, the calculated values are widely different from the experimental values of Hsieh and Colella [1]. This disagreement increases as the temperature is decreased from 300 to 105 K, as is also evident from figure 1.

For the KB model $n_z = 10 \times 10^{-6}$, $\theta_{0z} = 7$ K and $\theta_{mz} = 1000$ K. Using these parameters and expression (4), we have calculated the MSD along the *z* direction and these are plotted in figure 1. The calculated values are in much better agreement with the experimental values than those given by Komatsu model over most of the temperature range. However, the values of MSD particularly at low temperatures, i.e. less than 60 K, are lower than the experimental values and the difference becomes a maximum at $T = 0$ K being about (–18%). At high temperatures, also, the calculated values are

somewhat different from the experimental values and the difference is maximum at $T = 300$ K about (+18%).

Using expression (3), we find that $\theta_{0z} = 60$ K and $\theta_{mz} = 840$ K gives the calculated values of MSD that are in better agreement with the experimental values given by Hsieh and Colella [1] as shown in figure (1). The maximum deviation at $T = 0$ K is about -5% and at $T = 300$ K is about $+10\%$. In figure 1 we have also plotted the two-dimensional and three-dimensional contributions to $\langle u_z^2 \rangle$ based on our model. $\langle u_z^2 \rangle_{3D}$ is the contribution corresponding to first term of $g_i(\nu)$, i.e. $A_i \nu_i^2$ when $i = z$ of equation (1), while $\langle u_z^2 \rangle_{2D}$ is the contribution corresponding to second term, i.e. $B_z \nu_z$ from equation (1), to $\langle u_z^2 \rangle$. As is evident from figure (1), the two dimensional, $\langle u_z^2 \rangle_{2D}$, contribution to the MSD is much larger than the three-dimensional, $\langle u_z^2 \rangle_{3D}$, contribution at all the temperatures. However the ratio $\langle u_z^2 \rangle_{2D} / \langle u_z^2 \rangle_{3D}$ while at $T = 0$ K is about 25, at $T = 300$ K is about 3. The two-dimensional modes, therefore, predominate over the three-dimensional modes over the entire temperature range.

We may also point out that for graphite, the linear temperature-dependence of $\langle u_z^2 \rangle$ does not set in up to 300 K. Even in the three-dimensional isotropic Debye model, the linear temperature-dependence comes in only when temperature becomes much greater than θ_D . The value of θ_D quoted by Hsieh and Colella [1] is 572 K, which does not satisfy the condition for linearity in $\langle u_z^2 \rangle$ against T for graphite even at 300 K. The contributions of immediately higher-order non-linear term (T^2) is about 61% of the linear term at 100 K which becomes about 21% at 200 K and about 10% at 300 K of the corresponding linear terms. Only at the temperature 700 K, does the contribution of higher-order term become equal to 2%.

Making use of expression (7) with $\theta_{0z} = 60$ K and $\theta_{mz} = 840$ K, the second-order Doppler shifts along the c axis, $\delta_{T,z}$, have been calculated at various temperatures. In figure 2(a) are shown the calculated values for the second-order Doppler shift relative to its value at 293 K, Δ_{SOD} , in the temperature range 293–743 K and they are compared with the corresponding measured results at 293, 473 and 743 K [7]. The agreement between the two is good. In figure 2(b) are shown the contributions of two dimensional and three-dimensional modes to $\delta_{T,z}$ at various temperatures in the temperature range 0–743 K. As is evident from the figure, the contributions of two-dimensional modes are predominant over the entire temperature range.

In figure 3 the calculated values of the specific heat of graphite are shown in the temperature range 10–300 K, using $\theta_D = 572$ K and our model for all the dynamical modes. In our model we find that the characteristic parameters $\theta_{0xy} = 60$ K and $\theta_{mxy} = 2600$ K yield the calculated values of the temperature-dependent specific heat in agreement with the experimental values [8], which are also plotted in the figure. As is evident from figure 3, the calculated values of the specific heat using $\theta_D = 572$ K are very much different from the experimental values in the temperature range 40–300 K, the calculated values being much larger than the corresponding experimental results. In the same temperature range, the calculated values based on our model are in much better agreement with the corresponding experimental data. Also plotted in figure 3 are the contributions of z -modes and xy -modes from our model and, as expected, we find that z -mode contribution is dominant (80%) over most of the temperature range. It may be noted that if one takes the ($\frac{1}{3}$) values of the specific heat given by $\theta_D = 572$ K to represent the z -mode contribution only, the calculated values will still be higher than the corresponding experimental results over the temperature range 60–200 K and much lower than the experimental results at lower temperatures. Any model to represent the contribution of xy -modes that may bring the theoretical contribution nearer the experimental results at low temperatures will yield much higher values of specific heat at

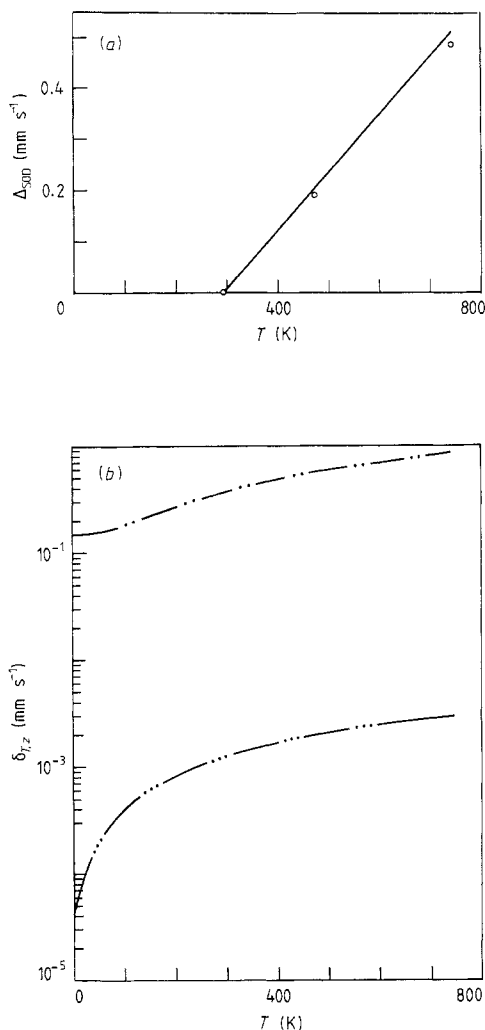


Figure 2. (a) Comparison of the calculated temperature-dependent second-order Doppler shift perpendicular to the basal plane in graphite relative to its value at 293 K with the experimental results in the temperature range 293–743 K. (b) contributions of two-dimensional (— · — · —) and three-dimensional (— · · · —) modes to the z-component of second-order Doppler shift in graphite in the temperature range 0–743 K.

higher temperatures. This would result in large disparity between the experimental and theoretical values at higher temperatures.

From our study, we conclude that the observed anisotropic mean-square displacement of bulk atoms of graphite can be explained using a model that explicitly takes into account the presence of two-dimensional planes in graphite. The model also yields consistent values for the temperature-dependent second-order Doppler shift and specific heat. Further, the effect of two-dimensional modes is found to be dominant at all the temperatures.

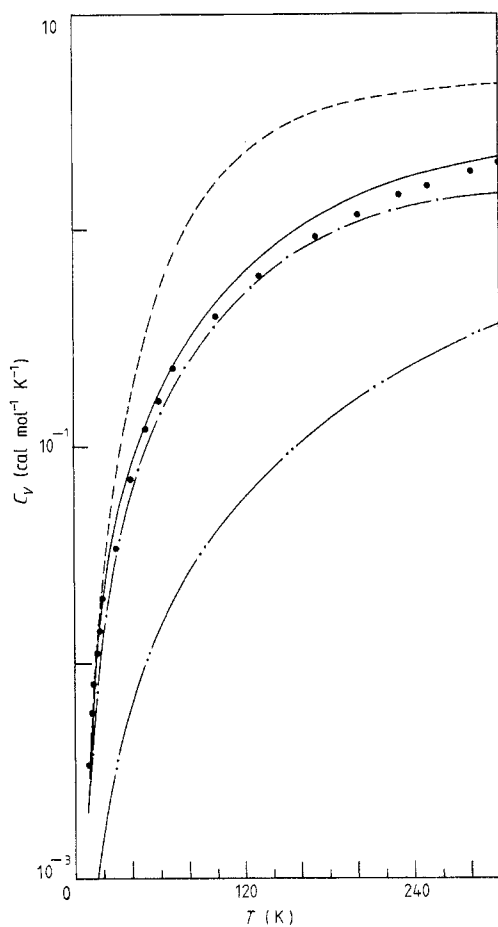


Figure 3. Specific heat of graphite. ● represents the experimental points. ---- denotes the specific heat using $\theta_D = 572$ K and — represents the specific heat using our model. Also shown are the z- and xy-mode contributions to the specific heat represented by —·— and —··— respectively.

References

- [1] Hsieh S M and Colella R 1987 *Solid State Commun.* **63** 47
- [2] Krumhansl J and Brooks H 1953 *J. Chem. Phys.* **21** 1663
- [3] Komatsu K 1955 *J. Phys. Soc. Japan* **10** 346
- [4] Chen H H and Yiu C L 1974 *Phys. Lett.* **48A** 77
- [5] Potzel W, Adlassnig W, Narger Ulrike, Obenhuber Th, Riski K and Kalvius G M 1984 *Phys. Rev. B* **30** 4980
- [6] Ludstek Von A 1972 *Acta Crystallogr. A* **28** 59
- [7] Pollak H, de Coster M and Amelinckx S 1962 *Proc. Second Mössbauer Conf., Paris, September 3–16 1961* ed. A Schoen and D M J Compton (New York: Wiley) p 112
- [8] DeSorbo W and Tyler W W 1953 *J. Chem. Phys.* **21** 1660
- [9] Keesom P H and Pearlman N 1955 *Phys. Rev.* **99** 1119
- [10] Boato G, Cantini P, Salvo C, Tatarek R and Terreni S 1982 *Surf. Sci.* **114** 485
- [11] Tewari S P and Silotia P 1989 *J. Phys.: Condens. Matter* **1** 5165–70
- [12] Albanese G, Bridelli M G and Deriu A 1984 *Biopolymers* **23** 1481
- [13] Tewari S P and Swaminathan K 1986 *Hyperfine Interact.* **29** 1385
- [14] Swaminathan K and Tewari S P 1986 *Polymer Communications* **27** 128